iScience

CellPress

Article

Werner Syndrome Helicase Is Required for the Survival of Cancer Cells with Microsatellite Instability

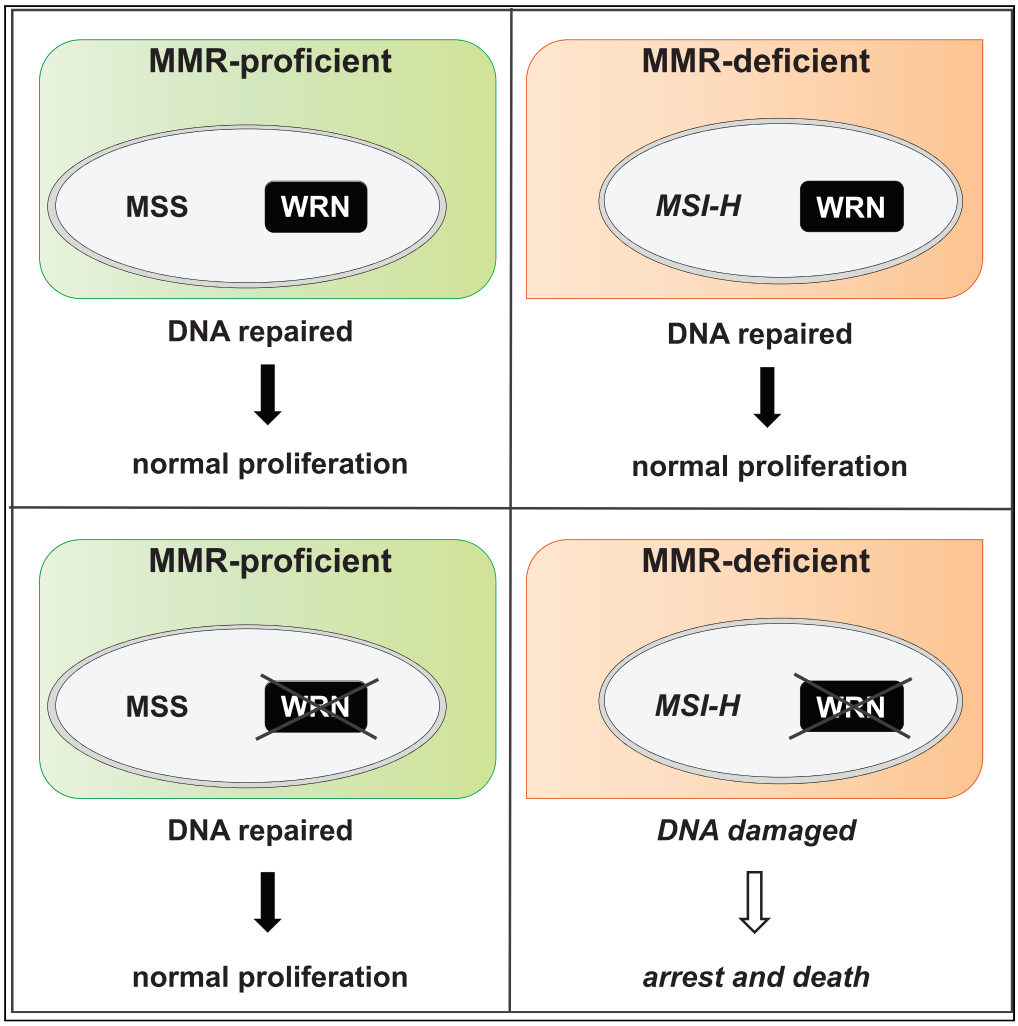

Lorn Kategaya, Senthil K. Perumal, Jeffrey H. Hager, Lisa D. Belmont

lkategaya@gmail.com (L.K.)
lbelmont@ideayabio.com (L.D.B.)

HIGHLIGHTS

Decreasing WRN expression negatively affects the survival of MSI-H cells

An increase in DSBs and altered cell cycles preceded MSI-H viability loss

WRN helicase inhibitors may be a beneficial therapy for patients with MSI-H cancers

Kategaya et al., iScience *13*, 488–497
March 29, 2019 © 2019 The Authors.
https://doi.org/10.1016/j.isci.2019.02.006

iScience

CellPress

Article

Werner Syndrome Helicase Is Required for the Survival of Cancer Cells with Microsatellite Instability

Lorn Kategaya,[1,3,*] Senthil K. Perumal,[1] Jeffrey H. Hager,[2] and Lisa D. Belmont[1,*]

SUMMARY

Werner syndrome protein (WRN) is a RecQ enzyme involved in the maintenance of genome integrity. Germline loss-of-function mutations in *WRN* led to premature aging and predisposition to cancer. We evaluated synthetic lethal (SL) interactions between WRN and another human RecQ helicase, BLM, with DNA damage response genes in cancer cell lines. We found that WRN was SL with a DNA mismatch repair protein MutL homolog 1, loss of which is associated with high microsatellite instability (MSI-H). MSI-H cells exhibited increased double-stranded DNA breaks, altered cell cycles, and decreased viability in response to *WRN* knockdown, in contrast to microsatellite stable (MSS) lines, which tolerated depletion of WRN. Although WRN is the only human RecQ enzyme with a distinct exonuclease domain, only loss of helicase activity drives the MSI SL interaction. This SL interaction in MSI cancer cells positions WRN as a relevant therapeutic target in patients with MSI-H tumors.

INTRODUCTION

Clinical success of poly (ADP-ribose) polymerase PARP inhibitors in BRCA-deficient cancers has triggered immense interest in identifying new synthetic lethal (SL) partners that could be exploited as drug targets for cancer therapy (Lord and Ashworth, 2017). In a *Saccharomyces cerevisiae* genetic screen to uncover SL interactions between tumor suppressor genes and drug targets, *SGS1*, which encodes the only *S. cerevisiae* RecQ helicase, was found to interact with several genes whose products Mus81, Rad17, Ubc9, Srs2, Mre11, Rad24, and TOP3 are heavily involved in DNA damage repair (DDR) (Srivas et al., 2016). An earlier SL screen with Sgs1 identified the SLX (synthetic lethal) gene family and other gene products that are important for DDR processes (Mullen et al., 2001). Unlike *S. cerevisiae*, there are five human RecQ helicases: BLM, WRN, RECQL, RECQL4, and RECQ5; BLM is considered the human ortholog of Sgs1 (Lillard-Wetherell et al., 2005). BLM was proposed to be SL with cell cycle regulators that are activated following DDR, checkpoint kinases 1 and 2 (Srivas et al., 2016).

RecQ helicases are ATP-dependent enzymes capable of unwinding a variety of DNA structures that are involved in DNA replication and recombination reactions (Wu et al., 2000). RecQ helicases contain signature motifs conserved in DNA and RNA helicases that have significant homology within the *E. coli* RecQ helicase domain (Wu et al., 2000). BLM and WRN enzymes are known to process G4 quadruplexes, Holliday junctions, forked DNA, and bubble DNA in addition to simple duplex DNA with single-stranded DNA (ssDNA) overhang structures. All these enzymes catalyze unwinding of DNA structures with a 3′-to-5′ directionality while also tracking on ssDNA, 3′-to-5′ (Wu et al., 2000). In addition to the helicase function mediated through the C-terminal domain, WRN is the only RecQ helicase known to possess 3′-to-5′ exonuclease activity (Croteau et al., 2014).

Germline mutations in *BLM, WRN,* and *RECQL4* are responsible for Bloom syndrome, Werner syndrome (WS), and Rothmund-Thomson and RAPADILINO syndromes, respectively (Karow et al., 2000). These syndromes are characterized by spontaneous chromosome instability, increased frequency of sister chromatid exchange (BLM), predisposition to cancer, and premature aging (WRN), phenotypes that highlight the important roles these enzymes play in DNA replication and DDR pathways (Karow et al., 2000). These three enzymes are also involved in resolution of stalled replication and transcription intermediates. RecQ helicase-mutated syndromes overlap but are also distinct symptomatically, when their expression is altered or lost. This suggests that they may have overlapping and distinct functions depending upon the timing and site of expression in cells as well as their interactions with other DNA replication and repair proteins and post-translational modifications. Given the established roles of the RecQ helicases in DNA replication

[1]Biology Department, IDEAYA Biosciences, 7000 Sierra Point Boulevard, South San Francisco, CA 94080, USA

[2]Biology Department, IDEAYA Biosciences, 3033 Science Park Road, Suite 250, San Diego, CA 92121, USA

[3]Lead Contact

*Correspondence: lkategaya@gmail.com (L.K.), lbelmont@ideayabio.com (L.D.B.)

https://doi.org/10.1016/j.isci.2019.02.006

This is an open access article under the CC BY-NC-ND license (http://creativecommons.org/licenses/by-nc-nd/4.0/).

and repair, we set out to identify SL partners using a candidate gene approach. We focused on *BLM*, due to its close homology to yeast *Sgs1*, and on *WRN* because of its unique exonuclease domain. SL interactions of *BLM* and *WRN* were evaluated by measuring cell viability after simultaneous loss of (via CRISPR-Cas9 knockout [KO]) or decrease in (via small interfering RNA [siRNA]) *BLM* or *WRN* and potential SL partners involved in the DDR pathways. In addition, we used small-molecule inhibitors to evaluate potential SL interactions.

WRN and MLH1 co-depletion by RNAi exhibited a significant combination effect on decreasing the viability of cells. MLH1 is a mismatch repair (MMR) protein that senses DNA mismatches during the replication phase of the cell cycle. Expression of MLH1 and other MMR proteins can be decreased, either through loss-of-function mutations or by promoter hypermethylation. MMR-deficient cells and tumors display high microsatellite instability (MSI-H). In this study, we report that MSI-H cells depend on WRN for their survival and that inhibiting WRN helicase activity may represent a unique therapeutic strategy for patients with cancer with MSI-H tumors.

RESULTS

Dual siRNA Knockdown of *WRN* and *MLH1* Decreases Cell Proliferation

BLM participates in homologous recombination-dependent (HR) repair, whereas it is thought that WRN participates in both HR and non-homologous end joining (NHEJ). In addition, it has been postulated that *BLM* is synthetic lethal with *CHEK1* and *CHEK2* based on simultaneous low BLM and CHEK1/2 expression in samples from patients with superior clinical outcomes (Srivas et al., 2016). We set out not only to test the *BLM and CHEK* SL interactions but also to test if the SL interaction is specific to *BLM* or if this extends to *WRN*. In addition, we tested other potential SL interactions with clinically relevant DDR genes (Figure S1 and Table S1). The following three experimental approaches were employed: (1) inhibiting PARP1/2, ATM, CHEK1, CHEK1/2, and DNAPK activities in isogenic HAP1 cell lines mutant or wild-type (WT) for BLM or WRN; (2) transfecting HAP1 parental and WRN/BLM KO cells with siRNAs of potential SL partners or transfecting WRN and BLM siRNAs into HAP1 KO cells of potential SL partners; and (3) dual siRNA experiments that involve transfecting siRNAs individually or as pairs in the non-small-cell lung cancer cell line, A549.

The HAP1 isogenic pair data are summarized in Table S1. For most pairwise perturbations, there was no effect on cell proliferation when the expression of BLM or WRN and a potential SL partner was deleted or decreased. Another outcome was that the result observed was context dependent. For example, PARP inhibition was synergistic in both HAP1 BLM and WRN KO cells compared with the parental but not when *BLM* and *WRN* were knocked down in another cell line (Hs578T) followed by treatment with PARP inhibitors, indicating cellular context dependency. The third and sought outcome, we observed only when *WRN* and *MLH1* expression was reduced, leading to a significant reduction in proliferation of A549 cells (Figure 1A). Three siRNAs targeting *MLH1* showed efficient knockdown (KD) of MLH1 transcript and protein as did the BLM and WRN siRNA on BLM and WRN expression, respectively (Figures S2A and 2B). The interaction between *WRN* and *MLH1* consistently exhibited a greater than additive effect (Figure 1A) based upon excess over Bliss score analysis (Greco et al., 1995). This synergy was specific to *WRN* as dual KD of *BLM* and *MLH1* did not exhibit a significant effect on cell proliferation (Figure 1A).

Defects in several MMR genes are associated with hereditary non-polyposis colon cancer (HNPCC) or Lynch syndrome, which are characterized by microsatellite instability. Mutations of PMS1, MLH1, and MSH2 have been implicated in HNPCC (Lynch and Lynch, 2000). During MMR, MSH2 exists in a complex with MSH6 and MLH1 exists in a complex with PMS2. When MSH2 or MLH1 expression is reduced, MSH6 and PMS2 are destabilized suggesting that MSH2 and MLH1 are core components of the protein complexes that detect DNA mismatches. Dual KD of WRN and the other genes involved in mismatch recognition pathways, *MSH2, PMS1, and PMS2*, did not phenocopy the synergy observed in WRN and MLH1 dual KD (Figure S3). These results imply that, at least in studies using transient RNAi-mediated mRNA KD and short-term proliferation assays, WRN is synthetically lethal with MLH1 but not the other proteins of MMR core complexes.

MMR-Deficient Cell Lines Are Sensitive to WRN Knockdown

To understand the WRN and MLH1 SL interaction in the broader context of MMR-deficient/MSI-H colorectal cancer, we tested WRN dependency in MMR-deficient cells that exhibit MSI-H versus MMR-proficient

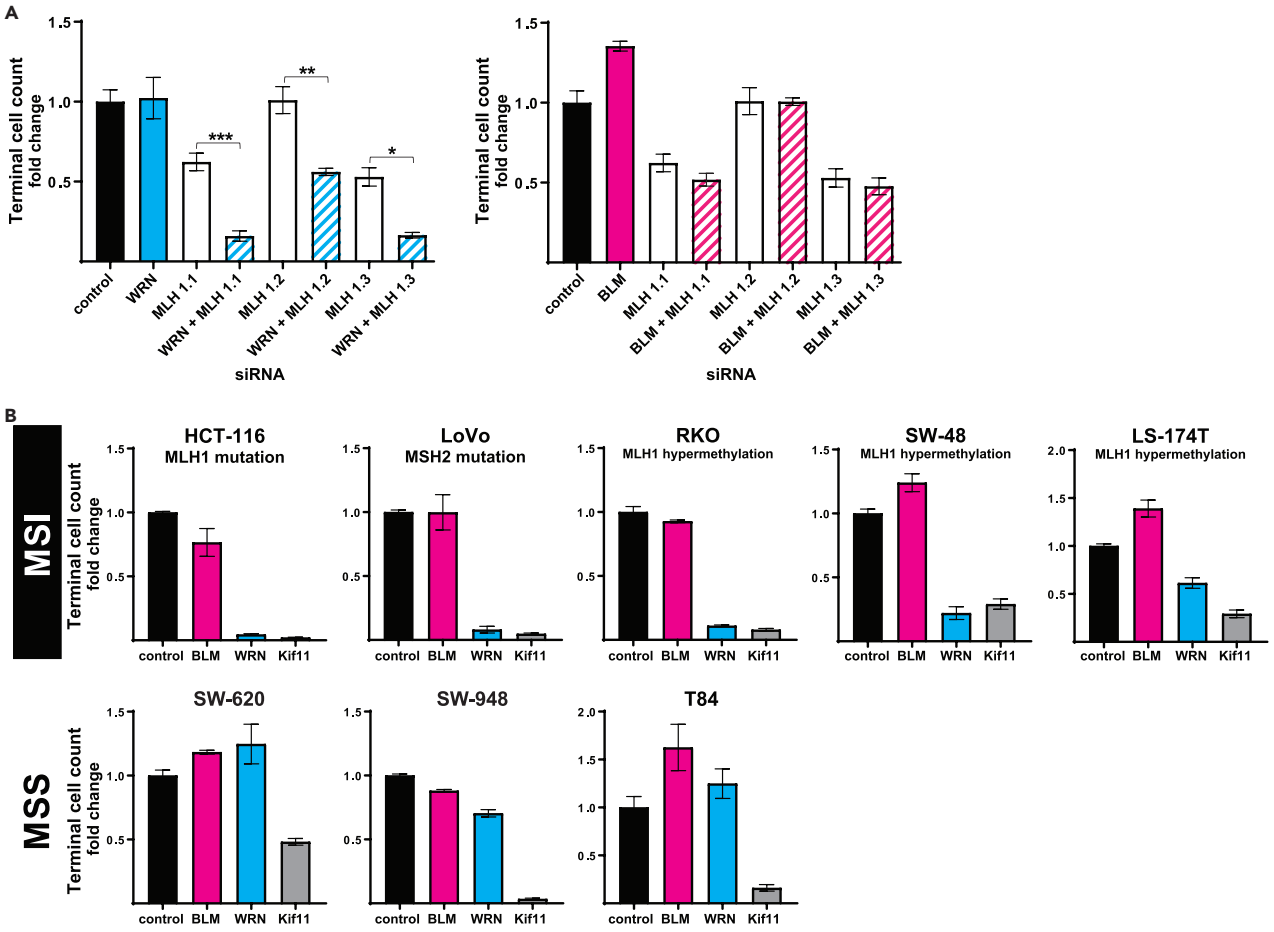

Figure 1. MSI cell lines are sensitive to WRN knockdown.

(A) Terminal cell counts in a 10-day proliferation assay after transfection of A549 cells with control, WRN (left) or BLM (right), and three independent MLH1 siRNAs. Excess over Bliss for WRN and MLH siRNA 1 (MLH1.1) = 0.48, WRN and MLH siRNA 2 (MLH1.2) = 0.47, and WRN and MLH siRNA 3 (MLH1.3) = 0.38. One-way ANOVA ***$p \leq 0.0001$, **$p \leq 0.001$, *$p \leq 0.01$.

(B) Graphs showing terminal cell counts in 7- to 10-day proliferation assays following transfection of five MSI cell lines (HCT116, LoVo, RKO, SW48, LS174T) and three MSS cell lines (SW620, SW948, and T84). Cells were transfected with control, BLM, WRN, or Kif11 (essential gene and positive control for decreased proliferation). Data are representative of three biological experiments. Error bars represent SEM.

cells that are microsatellite stable (MSS) (Figure 1B). Interestingly, we found that all five MSI-H cell lines tested were sensitive to *WRN* KD in 7- or 10-day viability assays. The loss in proliferation with *WRN* siRNA was comparable to that of a pan-essential gene, *KIF11*. In contrast, MSS cell lines were insensitive to *WRN* KD. Efficient KD was confirmed using RT-PCR (Figure S2C). This observation was supported by results from two large-scale dropout screens in which WRN was found to be essential in MMR-deficient/MSI-H cell lines derived from cancers of the large intestine, endometrium, and stomach (McDonald et al., 2017; Tsherniak et al., 2017). None of the other four human RECQ helicases tested in these screens showed this MSI SL interaction, thus it is unique to WRN. Notably, WRN was essential in LoVo, an MSI-H cell line that harbors loss-of-function mutation in *MSH2* and retains the WT *MLH1*. This suggests that WRN is broadly SL with a defect in MMR or the downstream MSI phenotype, not just MLH1. However, this result contradicts the dual siRNA experiments wherein MSH2 was not SL with WRN (Figure S3A). One explanation for the lack of synergy is that transient siRNA KD, in some cases, may not be sufficient when probing SL interactions with phenotypes that only emerge after extended reduction of protein levels.

Requirement for the structure-specific flap endonuclease, FEN1, was recently reported in MSI-H cell lines (Ward et al., 2017). Further investigation demonstrated that this was likely due to an SL relationship between FEN1 and MRE11, a protein that is frequently compromised in MSI-H cell lines because of one or

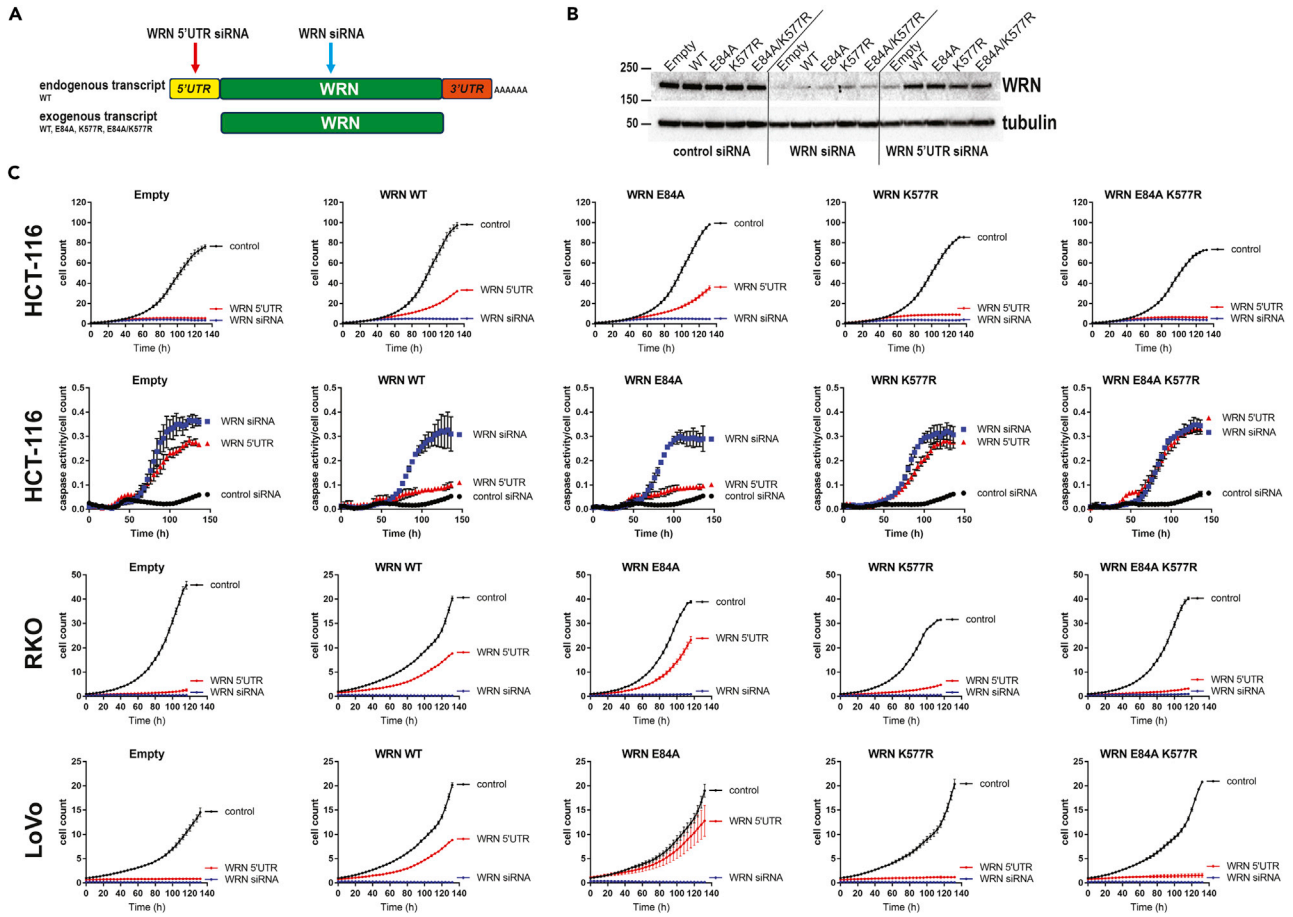

Figure 2. WRN Helicase Domain Rescues the WRN Knockdown Loss of Proliferation Phenotype in MSI Cells

(A) Schematic representation of endogenous WRN wild-type (WT) and siRNA-resistant exogenous transcripts (WT, E84A [exonuclease-dead], K577R [helicase-dead], and E84A/K577R [enzymatically dead]). The endogenous transcript contains a 5′ UTR that can be selectively targeted by an siRNA (WRN 5′UTR siRNA). An internally targeting siRNA (WRN siRNA) leads to a decrease in both endogenous and exogenous WRN transcripts.

(B) WRN and tubulin immunoblots of HCT116 rescue cells transfected with the indicated siRNAs. Numbers on blots indicate where molecular weight (kD) bands of protein ladder would be.

(C) Growth curves of MSI (HCT116, RKO, LoVo) cells transfected with the indicated siRNAs. Relative caspase activity (raw caspase activity/cell number) over time in HCT116 rescue cell lines transfected with the indicated siRNAs (second row). Error bars represent SEM. Data are representative of three biological experiments.

two deleted thymidine residues of a poly T tract that resides in intron 4. Because all MMR-deficient, MSI-H cell lines sensitive to WRN KD also harbor homozygous mutations in MRE11 (Figure 1B) we tested whether loss of MRE11 is in fact the driver of the SL interaction with WRN. An MSI-H cell line wherein MSH6 is lost, DLD-1, has one WT copy of MRE11, resulting in normal protein levels and function. DLD-1 cells are insensitive to WRN KD alone, and knocking down MRE11 did not sensitize DLD-1 cells to WRN loss (Figure S4). Furthermore, re-expressing MRE11 in WRN-sensitive MSI cell lines (Figure S5B) did not rescue the WRN siRNA phenotype (Figure S5C), suggesting that loss of MRE11 function is not responsible for the strict WRN dependency in MSI-H cell lines.

To further elucidate the mechanism by which reduction of MLH1 results in dependency on WRN, we also re-expressed MLH1 in HCT116 and RKO cell lines. Surprisingly, MLH-1 expression did not rescue the WRN KD phenotype in MLH1 mutant cell lines. To demonstrate that MLH1 re-expression levels were sufficient to restore MMR function, we evaluated the sensitivity of these cells to 6-thioguanine (6-TG). MMR-proficient cells are sensitive, whereas MMR-deficient cells are resistant to 6-TG (Yan et al., 2003). RKO MLH1 re-expressing cells were more sensitive to 6-TG compared with RKO parental cells, indicative of MLH1-mediated functional rescue of MMR (Figure S5D). MLH1 KD increases telomeric sequence insertions

intrachromosomally (Jia et al., 2017) and induces MSI (Bailis et al., 2013), which may explain why we observe synthetic lethality when both WRN and MLH1 expression are decreased, but not when MLH1 is re-expressed, as the genomic alterations downstream of MLH1 loss are most likely irreversible. Alternatively, it is likely that restoration of MMR is partial as RKO cells possess frameshift mutations in other MMR genes (*MLH3* and *MSH6*) that result in the deletion of their carboxy-terminal domains (Barretina et al., 2012). Notably, MMR and MSI are rescued in HCT116 cells only when both MLH1 and MSH3 expression are restored via chromosomal transfer (Haugen et al., 2008). Taken together, these data indicate that the cellular dependency of WRN in cells with MSI is not readily rescued by acute reconstitution of only MLH1 function.

WRN Helicase Domain Rescues WRN Knockdown Phenotype in MSI Cells

WRN is the only human RecQ family enzyme that has both a helicase activity and an exonuclease activity, and these activities arise from two different domains in the protein. WS is caused by mutations in *WRN* that typically result in complete loss of function of both domain activities. However, the characterization of one non-pathogenic human WRN variant, R834C, demonstrated a 90% loss of helicase activity but no loss of exonuclease function, suggesting that the intact exonuclease function is sufficient to prevent WRN syndrome (Kamath-Loeb et al., 2017). We set out to determine which domain is required for the WRN MSI SL interaction to define a small-molecule therapeutic targeting strategy. We generated cell lines constitutively expressing siRNA-resistant WT, exonuclease-dead (E84A), helicase-dead (K577R), and enzymatically dead (E84A/K577R) WRN proteins. The loss of enzymatic activity with these WRN mutations has been previously characterized. It is important to note that the two enzymatic activities of WRN were effectively decoupled from one another to provide an unbiased assessment of the domain specificity of WRN MSI SL interaction. ATPase activity and unwinding activity of helicases are tightly coupled, and hence by mutating K577 of the Walker A domain of WRN involved in ATP binding and hydrolysis, the unwinding activity is completely abolished (Iannascoli et al., 2015). This generated a mutant that is completely devoid of helicase activity without perturbing the nuclease activity. We transfected the cells with siRNA targeting the 5′ untranslated region (UTR) to target endogenous WRN or in exon 8 (to target endogenous and exogenously expressed WRN mRNA) (Figure 2A). An siRNA-resistant pool of WRN was detected by western blot using the 5′UTR siRNA demonstrating discriminatory WRN KD as designed (Figures 2B and S6A).

KD with both WRN siRNAs decreased the proliferation of the negative control cell lines ("empty"). We observed partial to almost complete rescue with WT and exonuclease-dead WRN in cells transfected with the 5′UTR siRNA (Figure 2C). In contrast, the helicase-dead and enzymatically dead WRN did not rescue the loss of proliferation observed with the 5′UTR siRNA. We also found that WRN KD increased the relative activity of caspases 3 and 7 in HCT116 cells, consistent with the loss of viability being at least in part through apoptosis (Figure 2C). Consistent with the rescue of proliferation, exogenous WT and exonuclease-dead WRN, and not helicase-dead mutants, rescued the increase in caspase activity in cells transfected with the 5′UTR siRNA. These results indicate that loss of helicase activity, and not the exonuclease activity of WRN, drives the SL interaction between WRN and MSI.

WRN Knockdown Increases DSB and Alters the Cell Cycle of MSI Cells

To understand the mechanism by which WRN KD causes loss of viability in MSI-H cells, we harvested cells 24, 48, and 72 h after siRNA transfection and monitored DNA double-strand breaks and the G1 to S checkpoint by immunodetection of γH2AX and p21, respectively (Figure 3). Compared with control siRNA, HCT116 (Figure 3A) and RKO (Figure S6A) cells transfected with WRN siRNA showed greater number of positive staining cells for both γH2AX and p21. Consistent with the lack of viability effects, SW620 (MSS) cells did not show a change in γH2AX levels upon WRN KD (Figure S6). p21 immunoreactivity was not detected in SW620 cells, the only cell line among the three tested that carries mutant *TP53*. p21 is a p53 target gene, and thus functional p53 might be required for WRN KD-induced p21 expression. Interestingly, most MSI-H cell lines except DLD-1 cells are WT for *TP53,* whereas MSS cell lines are mostly mutant for *TP53* (Ahmed et al., 2013). However, examination of a larger panel of cell lines (Cancer Dependency Map portal) shows that MSI-H cells are sensitive to WRN KD or KO regardless of TP53 mutation status (Tsherniak et al., 2017).

The increase in p21 levels following WRN loss in MSI cells led us to measure cell cycle changes in these cells. Flow cytometry analyses revealed a decrease in number of cells in S-phase, consistent with elevated levels of p21. We also observed a decrease in cells in M-phase and with 2N DNA and an increase in cells with 4N

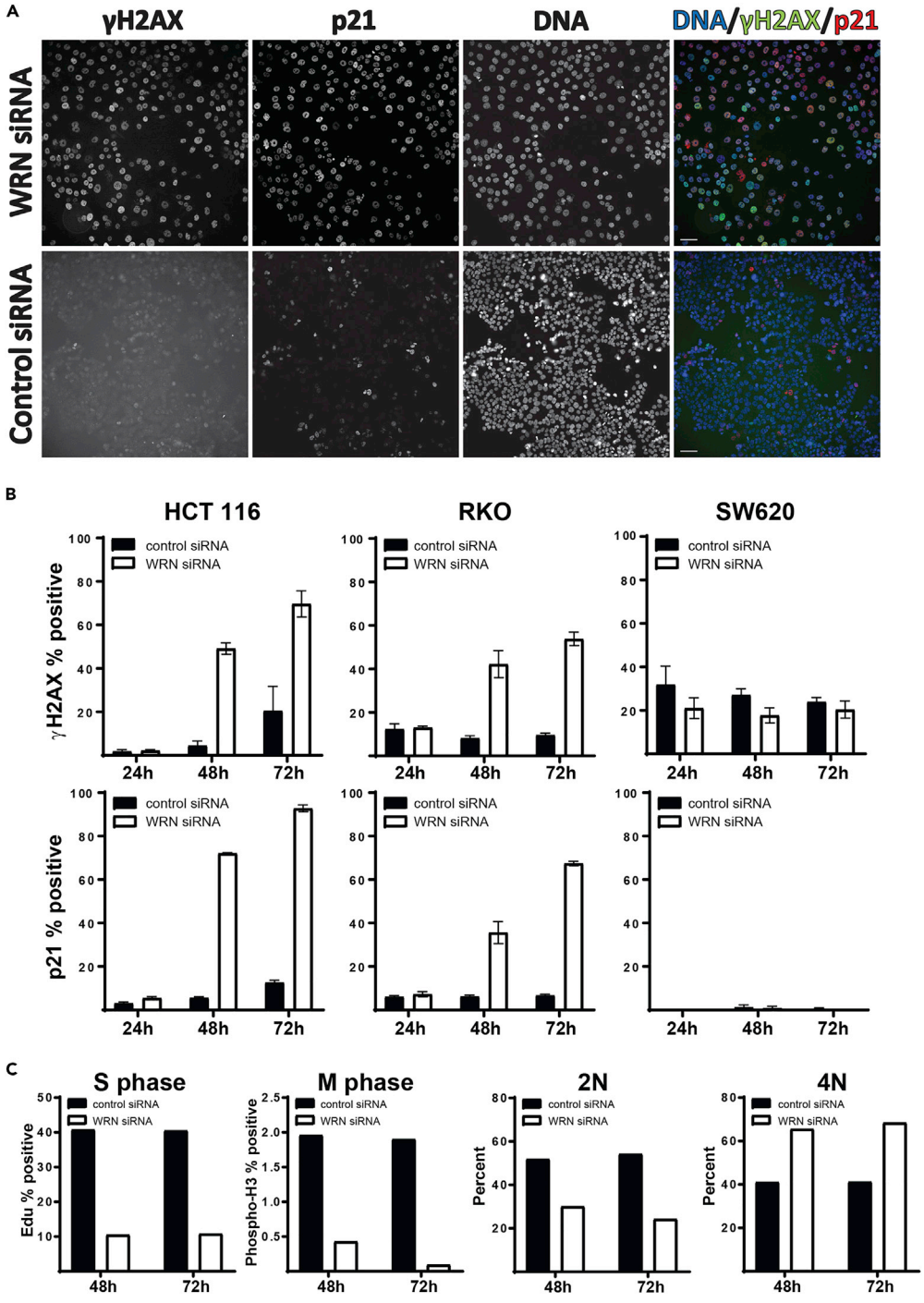

Figure 3. WRN Knockdown Increases γH2AX and p21 Levels and Alters the Cell Cycle of MSI Cells

(A) Representative immunofluorescence images of HCT116 cells transfected for 72 h with WRN (top row) or control (bottom row) siRNAs and incubated with Hoechst stain (DNA), p21, and γH2AX antibodies. Individual channels are shown in gray scale and overlay of all three channels in pseudo color. Scale bars, 50 μm.

(B) Graphs showing quantification of γH2AX and p21 staining from multiple images collected from two MSI cell lines (HCT116 and RKO) and one MSS cell line (SW620). Error represents STDEV.

(C) Flow cytometry data measuring cell cycles states of HCT116 cells 48 and 72 h after transfection with control or WRN siRNA. Data are representative of two biological experiments.

DNA (Figures 3C and S6B). An increase in cells with 4N DNA content can be due to G2 phase arrest, mitotic arrest, or mitotic slippage (Brito and Rieder, 2006). The decrease in phosphohistone H3-positive cells (Figure 3C) is not consistent with mitotic arrest, and the observation of high p21 levels favors the hypothesis that the cells have undergone mitotic slippage, exit of the mitotic state without completing mitosis, or cytokinesis resulting in entry into G1 with 4N DNA content.

DISCUSSION

RecQ helicases are involved in genome maintenance by playing key roles in DNA replication, recombination, and damage repair (Croteau et al., 2014). Exploiting human RecQ helicases as drug targets in cancers defective in DDR pathways is an attractive therapeutic strategy. Recent reports on inhibition of human BLM and WRN helicases suggest helicase-targeted therapy as viable approaches for small-molecule-mediated inhibition in the context of loss of synthetic lethal partner (Aggarwal et al., 2011, 2013a, 2013b; Banerjee et al., 2013; Nguyen et al., 2013). We examined SL interactions of *BLM* and *WRN* with the genes of clinically relevant human DDR proteins. Of the diverse DDR genes interrogated by acute RNAi-mediated KD, only MMR gene, *MLH1,* showed SL interaction with *WRN*. Further testing revealed that WRN was essential for survival of MMR deficient, and thus, microsatellite-unstable cells but not MMR-proficient MSS cells.

Domain-specific rescue experiments demonstrated that loss of WRN helicase activity, and not the exonuclease activity, is the driver of the SL interaction between WRN and MSI. It has been hypothesized that the helicase unwinds the duplex DNA and feeds the ssDNA to the nuclease-active site, which then exonucleolytically cleaves the DNA thereby improving the processivity of the helicase domain (Iannascoli et al., 2015). This has been supported by Replication Protein A (RPA) sequestering ssDNA generated by the helicase and increasing the processivity of WRN helicase (Lee et al., 2018). However, domain-specific rescue experiments indicate that the nuclease activity alone is insufficient to provide necessary WRN function to support growth and survival in MSI-H cancer cells, whereas the helicase domain can.

The involvement of WRN or other RecQ helicases in MMR pathways is not well understood. It has been proposed that WRN plays a role in an EXO1-independent pathway of mismatch repair in MSI-H cells (Kadyrov et al., 2006). DNA unwinding and Holliday junction remodeling activities of WRN would be able to directly remove the mismatch-containing fragment (Kadyrov et al., 2006). Mismatch-containing strand can be processed using the unwinding activities of WRN along with other MMR proteins, whereas in the EXO1-dependent pathway, the displaced strand would be degraded completely without a dependence on the helicase. In this model, MMR-deficient MSI-H cell lines in the absence of WRN would retain mismatched DNA, nicked DNA, as well as other non-canonical structures, which eventually generate DSB that accumulate leading to apoptosis.

We propose the following model to explain the WRN MSI interaction (Figure 4). In contrast to MSS cells, MSI cells have more non-canonical secondary DNA structures, such as single-stranded DNA loops and G4 quadruplexes. These can arise because of microsatellite repeats with CNC triplets, the G-quadruplex consensus sequence, or increased intrachromosomal telomere sequence insertions. WRN is among a small group of helicases that can effectively resolve G4 quadruplexes and has a higher affinity for diverse non-canonical DNA structures compared with BLM (Karow et al., 2000). We propose that in MSI-H cells, WRN is required to resolve non-canonical DNA structures generated from repeat sequences but not repaired by MMR proteins, either because of the increased number of structures or because WRN can resolve a larger array of DNA structures than BLM and the other RecQ helicases. MSI cells also show a decrease in homologous recombination (Mohindra et al., 2002). Considering WRN's role in NHEJ, loss of WRN decreases NHEJ, further limiting the cell's ability to repair double-stranded DNA breaks. Unresolved DNA damage after S-phase can result in G2 arrest or cell death. In addition, MMR defects impair telomere maintenance and WRN depletion leads to increased telomere fusions. The combination could result in entry into mitosis with fused telomeres that cannot be separated, resulting in cytoplasmic bridges and a failure in cytokinesis.

Synthetic lethality has the potential of delivering a large therapeutic window because the target is only essential in the absence of its SL partner, thus sparing non-tumorigenic normal cells. SL interactions are clinically actionable if one partner is amenable to pharmacological inhibition and the other partner has sufficient prevalence in cancer such that patients can be readily identified for treatment. The SL interaction

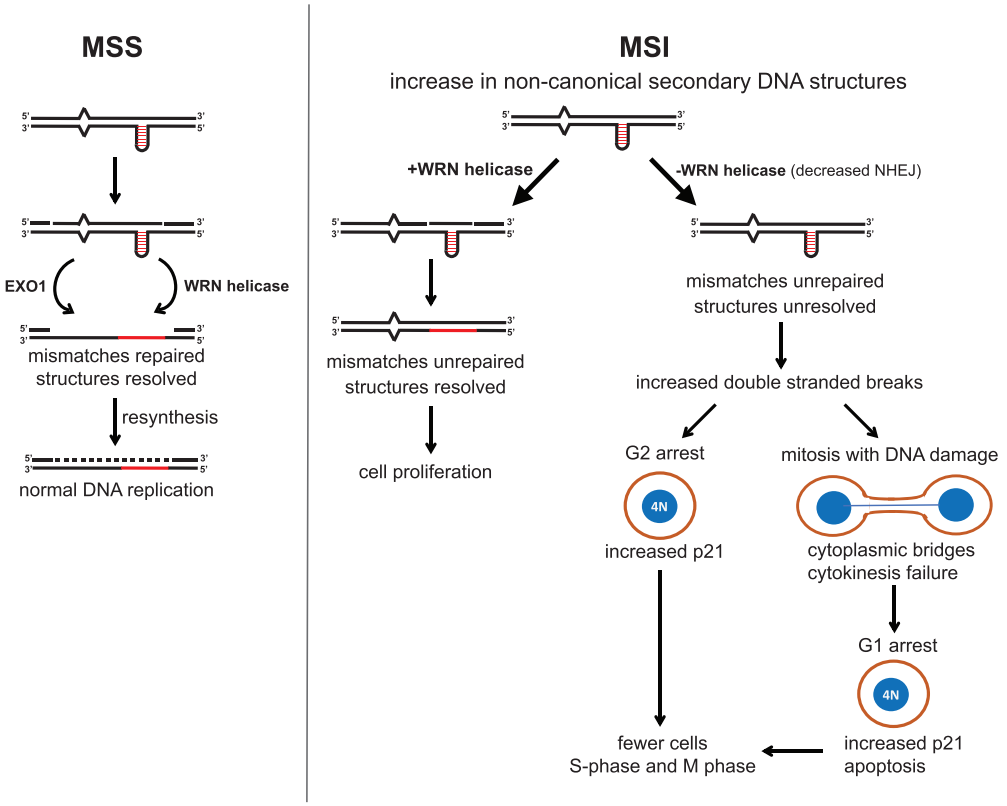

Figure 4. Model of WRN Function in MSS versus MSI cells

During replication, non-canonical DNA structures (hairpin) such as G4 quadruplexes in MSS cells are resolved by WRN and/or other helicases (left). DNA mismatches (open triangle) are repaired by MMR proteins. In MSI cells (right), there is an increase in non-canonical secondary structures creating a requirement for WRN for their resolution. When WRN expression is decreased, the replication machinery runs into the unresolved structures eventually leading to an increase in double-stranded breaks. Cells either arrest in G2 or proceed into mitosis with DNA damage. The latter cells fail to complete cytokinesis leading to G1 arrest or apoptosis.

between WRN and MSI fulfills both these requirements because WRN helicase function is not essential in MSS cells (Aumailley et al., 2015; Kamath-Loeb et al., 2017; Lombard et al., 2000) and MSI is evident in many types of cancers (Bonneville et al., 2017).

The anti-PD1 antibodies, pembrolizumab and nivolumab, were recently approved for use in patients with defects in MMR or MSI, independent of the tissue of origin. MSI occurs in multiple cancer types often when canonical MMR proteins are lost but can also occur when polymerase ε is mutated (Billingsley et al., 2015). Pembrolizumab exhibited 45% response rate in the targeted clinical population, and clinical response in these patients is thought to be a function of immunogenic, neo-antigen load that arises in MSI tumors. A WRN helicase inhibitor in combination with pembrolizumab has the potential to improve the rate and duration of response observed with pembrolizumab alone. WRN inhibition would directly target the tumor, whereas pembrolizumab stimulates the immune response against the tumor. The increased tumor cell death that we predict will arise by targeting WRN helicase in MSI tumors also has the potential to further stimulate the host immune response, mediating a cold to hot tumor phenotypic transition through an increased cGAS/STING-dependent type I interferon response. Our studies imply that a drug targeting the WRN helicase activity has potential as a monotherapy or in combination with immune checkpoint inhibitors, for patients bearing tumors with MSI.

Limitations of the Study

Although we propose a model (Figure 4) to explain, mechanistically, why MSI-H cells are dependent on WRN, we did not directly test the model.

METHODS

All methods can be found in the accompanying Transparent Methods supplemental file.

SUPPLEMENTAL INFORMATION

Supplemental Information can be found online at https://doi.org/10.1016/j.isci.2019.02.006.

ACKNOWLEDGMENTS

Hadia Lemar assisted with flow cytometry experiments. This research was funded by IDEAYA Biosciences Inc.

AUTHOR CONTRIBUTIONS

Conceptualization, L.K., S.K.P., J.H.H., and L.D.B.; Methodology: L.K.; Investigation: L.K. and S.K.P.; Writing, L.K., S.K.P., J.H.H., and L.D.B.

DECLARATION OF INTERESTS

J.H.H., L.D.B., and S.K.P. are employees and shareholders of IDEAYA Biosciences. L.K.owns IDEAYA shares. IDEAYA biosciences has filed one or more patent application directed to the subject matter of this publication.

Received: October 24, 2018
Revised: December 28, 2018
Accepted: February 6, 2019
Published: March 18, 2019

REFERENCES

Aggarwal, M., Banerjee, T., Sommers, J.A., and Brosh, R.M., Jr. (2013a). Targeting an Achilles' heel of cancer with a WRN helicase inhibitor. Cell Cycle *12*, 3329–3335.

Aggarwal, M., Banerjee, T., Sommers, J.A., Iannascoli, C., Pichierri, P., Shoemaker, R.H., and Brosh, R.M., Jr. (2013b). Werner syndrome helicase has a critical role in DNA damage responses in the absence of a functional fanconi anemia pathway. Cancer Res. *73*, 5497–5507.

Aggarwal, M., Sommers, J.A., Shoemaker, R.H., and Brosh, R.M., Jr. (2011). Inhibition of helicase activity by a small molecule impairs Werner syndrome helicase (WRN) function in the cellular response to DNA damage or replication stress. Proc. Natl. Acad. Sci. U S A *108*, 1525–1530.

Ahmed, D., Eide, P.W., Eilertsen, I.A., Danielsen, S.A., Eknaes, M., Hektoen, M., Lind, G.E., and Lothe, R.A. (2013). Epigenetic and genetic features of 24 colon cancer cell lines. Oncogenesis *2*, e71.

Aumailley, L., Garand, C., Dubois, M.J., Johnson, F.B., Marette, A., and Lebel, M. (2015). Metabolic and phenotypic differences between mice producing a Werner syndrome helicase mutant protein and Wrn null mice. PLoS One *10*, e0140292.

Bailis, J.M., Gordon, M.L., Gurgel, J.L., Komor, A.C., Barton, J.K., and Kirsch, I.R. (2013). An inducible, isogenic cancer cell line system for targeting the state of mismatch repair deficiency. PLoS One *8*, e78726.

Banerjee, T., Aggarwal, M., and Brosh, R.M., Jr. (2013). A new development in DNA repair modulation: discovery of a BLM helicase inhibitor. Cell Cycle *12*, 713–714.

Barretina, J., Caponigro, G., Stransky, N., Venkatesan, K., Margolin, A.A., Kim, S., Wilson, C.J., Lehar, J., Kryukov, G.V., Sonkin, D., et al. (2012). The cancer cell line encyclopedia enables predictive modelling of anticancer drug sensitivity. Nature *483*, 603–607.

Billingsley, C.C., Cohn, D.E., Mutch, D.G., Suarez, A.A., and Goodfellow, P.J. (2015). Polymerase varepsilon (POLE) mutations in endometrial cancer: clinical outcomes and implications for Lynch syndrome testing. Cancer *121*, 386–394.

Bonneville, R., Krook, M.A., Kautto, E.A., Miya, J., Wing, M.R., Chen, H.Z., Reeser, J.W., Yu, L., and Roychowdhury, S. (2017). Landscape of microsatellite instability across 39 cancer types. JCO Precis. Oncol. *1*, 1–15.

Brito, D.A., and Rieder, C.L. (2006). Mitotic checkpoint slippage in humans occurs via cyclin B destruction in the presence of an active checkpoint. Curr. Biol. *16*, 1194–1200.

Croteau, D.L., Popuri, V., Opresko, P.L., and Bohr, V.A. (2014). Human RecQ helicases in DNA repair, recombination, and replication. Annu. Rev. Biochem. *83*, 519–552.

Greco, W.R., Bravo, G., and Parsons, J.C. (1995). The search for synergy: a critical review from a response surface perspective. Pharmacol. Rev. *47*, 331–385.

Haugen, A.C., Goel, A., Yamada, K., Marra, G., Nguyen, T.P., Nagasaka, T., Kanazawa, S., Koike, J., Kikuchi, Y., Zhong, X., et al. (2008). Genetic instability caused by loss of MutS homologue 3 in human colorectal cancer. Cancer Res. *68*, 8465–8472.

Iannascoli, C., Palermo, V., Murfuni, I., Franchitto, A., and Pichierri, P. (2015). The WRN exonuclease domain protects nascent strands from pathological MRE11/EXO1-dependent degradation. Nucleic Acids Res. *43*, 9788–9803.

Jia, P., Chastain, M., Zou, Y., Her, C., and Chai, W. (2017). Human MLH1 suppresses the insertion of telomeric sequences at intra-chromosomal sites in telomerase-expressing cells. Nucleic Acids Res. *45*, 1219–1232.

Kadyrov, F.A., Dzantiev, L., Constantin, N., and Modrich, P. (2006). Endonucleolytic function of MutLalpha in human mismatch repair. Cell *126*, 297–308.

Kamath-Loeb, A.S., Zavala-van Rankin, D.G., Flores-Morales, J., Emond, M.J., Sidorova, J.M., Carnevale, A., Cardenas-Cortes, M.D., Norwood, T.H., Monnat, R.J., Loeb, L.A., et al. (2017). Homozygosity for the WRN helicase-inactivating variant, R834C, does not confer a Werner syndrome clinical phenotype. Sci. Rep. *7*, 44081.

Karow, J.K., Wu, L., and Hickson, I.D. (2000). RecQ family helicases: roles in cancer and aging. Curr. Opin. Genet. Dev. *10*, 32–38.

Lee, M., Shin, S., Uhm, H., Hong, H., Kirk, J., Hyun, K., Kulikowicz, T., Kim, J., Ahn, B., Bohr, V.A., et al. (2018). Multiple RPAs make WRN syndrome protein a superhelicase. Nucleic Acids Res. *46*, 4689–4698.

Lillard-Wetherell, K., Combs, K.A., and Groden, J. (2005). BLM helicase complements disrupted

type II telomere lengthening in telomerase-negative sgs1 yeast. Cancer Res. *65*, 5520–5522.

Lombard, D.B., Beard, C., Johnson, B., Marciniak, R.A., Dausman, J., Bronson, R., Buhlmann, J.E., Lipman, R., Curry, R., Sharpe, A., et al. (2000). Mutations in the WRN gene in mice accelerate mortality in a p53-null background. Mol. Cell. Biol. *20*, 3286–3291.

Lord, C.J., and Ashworth, A. (2017). PARP inhibitors: synthetic lethality in the clinic. Science *355*, 1152–1158.

Lynch, H.T., and Lynch, J. (2000). Lynch syndrome: genetics, natural history, genetic counseling, and prevention. J. Clin. Oncol. *18*, 19S–31S.

McDonald, E.R., 3rd, de Weck, A., Schlabach, M.R., Billy, E., Mavrakis, K.J., Hoffman, G.R., Belur, D., Castelletti, D., Frias, E., Gampa, K., et al. (2017). Project DRIVE: a compendium of cancer dependencies and synthetic lethal relationships uncovered by large-scale, deep RNAi screening. Cell *170*, 577–592.e10.

Mohindra, A., Hays, L.E., Phillips, E.N., Preston, B.D., Helleday, T., and Meuth, M. (2002). Defects in homologous recombination repair in mismatch-repair-deficient tumour cell lines. Hum. Mol. Genet. *11*, 2189–2200.

Mullen, J.R., Kaliraman, V., Ibrahim, S.S., and Brill, S.J. (2001). Requirement for three novel protein complexes in the absence of the Sgs1 DNA helicase in Saccharomyces cerevisiae. Genetics *157*, 103–118.

Nguyen, G.H., Dexheimer, T.S., Rosenthal, A.S., Chu, W.K., Singh, D.K., Mosedale, G., Bachrati, C.Z., Schultz, L., Sakurai, M., Savitsky, P., et al. (2013). A small molecule inhibitor of the BLM helicase modulates chromosome stability in human cells. Chem. Biol. *20*, 55–62.

Srivas, R., Shen, J.P., Yang, C.C., Sun, S.M., Li, J., Gross, A.M., Jensen, J., Licon, K., Bojorquez-Gomez, A., Klepper, K., et al. (2016). A network of conserved synthetic lethal interactions for exploration of precision cancer therapy. Mol. Cell *63*, 514–525.

Tsherniak, A., Vazquez, F., Montgomery, P.G., Weir, B.A., Kryukov, G., Cowley, G.S., Gill, S., Harrington, W.F., Pantel, S., Krill-Burger, J.M., et al. (2017). Defining a cancer dependency map. Cell *170*, 564–576.e16.

Ward, T.A., McHugh, P.J., and Durant, S.T. (2017). Small molecule inhibitors uncover synthetic genetic interactions of human flap endonuclease 1 (FEN1) with DNA damage response genes. PLoS One *12*, e0179278.

Wu, L., Davies, S.L., and Hickson, I.D. (2000). Roles of RecQ family helicases in the maintenance of genome stability. Cold Spring Harb. Symp. Quant. Biol. *65*, 573–581.

Yan, T., Berry, S.E., Desai, A.B., and Kinsella, T.J. (2003). DNA mismatch repair (MMR) mediates 6-thioguanine genotoxicity by introducing single-strand breaks to signal a G2-M arrest in MMR-proficient RKO cells. Clin. Cancer Res. *9*, 2327–2334.

ISCI, Volume *13*

Supplemental Information

Werner Syndrome Helicase Is Required for the Survival of Cancer Cells with Microsatellite Instability

Lorn Kategaya, Senthil K. Perumal, Jeffrey H. Hager, and Lisa D. Belmont

Table S1. Summary of genes tested, experiments carried out and results from a candidate approach mini-screen used to identify BLM and WRN synthetic lethal interactions. Related to Fig. 1.

Protein	Testing tools	Result
PARP	1. Olaparib on HAP1 BLM/WRN isogenic cells 2. Olaparib and talazoparib on BLM/WRN siRNA transfected Hs578T cells	Synergy observed was context dependent.
ATM	1. KU55933 and KU60019 on HAP1 BLM/WRN isogenic cells 2. BLM/WRN siRNA transfected ATM null cell lines (Hs695T, SKCO-1) 3. Dual siRNA in A549 cells	Synergy observed was context dependent.
DNAPK	1. NU7447 on HAP1 BLM/WRN isogenic cells 2. BLM/WRN siRNA transfected HAP1 DNAPK isogenic cells	No synergy
WEE1	MK-1775 on HAP1 BLM/WRN isogenic cells	No synergy
CHEK1	MK-8776 on HAP1 BLM/WRN isogenic cells	No synergy
CHEK1&2	AZD7762 on HAP1 BLM/WRN isogenic cells	No synergy
FANCD2	BLM/WRN siRNA transfected HAP1 FANCD2 isogenic cells	No synergy
FBXW7	1. BLM/WRN siRNA transfected HAP1 FBXW7 isogenic cells 2. Dual siRNA in A549 cells	No synergy
XRCC3	siRNA transfected HAP1 BLM/WRN isogenic cells	No synergy
RAD54B	siRNA transfected HAP1 BLM/WRN isogenic cells	No synergy
NBN	siRNA transfected HAP1 BLM/WRN isogenic cells	No synergy
LIG4	siRNA transfected HAP1 BLM/WRN isogenic cells	No synergy
DNA2	siRNA transfected HAP1 BLM/WRN isogenic cells	Synergy with BLM
ERCC5	siRNA transfected HAP1 BLM/WRN isogenic cells	No synergy
TP53BP1	siRNA transfected HAP1 BLM/WRN isogenic cells	No synergy
FANCM	siRNA transfected HAP1 BLM/WRN isogenic cells	Moderate synergy with BLM
MLH1	1. BLM/WRN siRNA transfected HAP1 MLH1 isogenic cells 2. Dual siRNA in A549 cells	Synergy with WRN

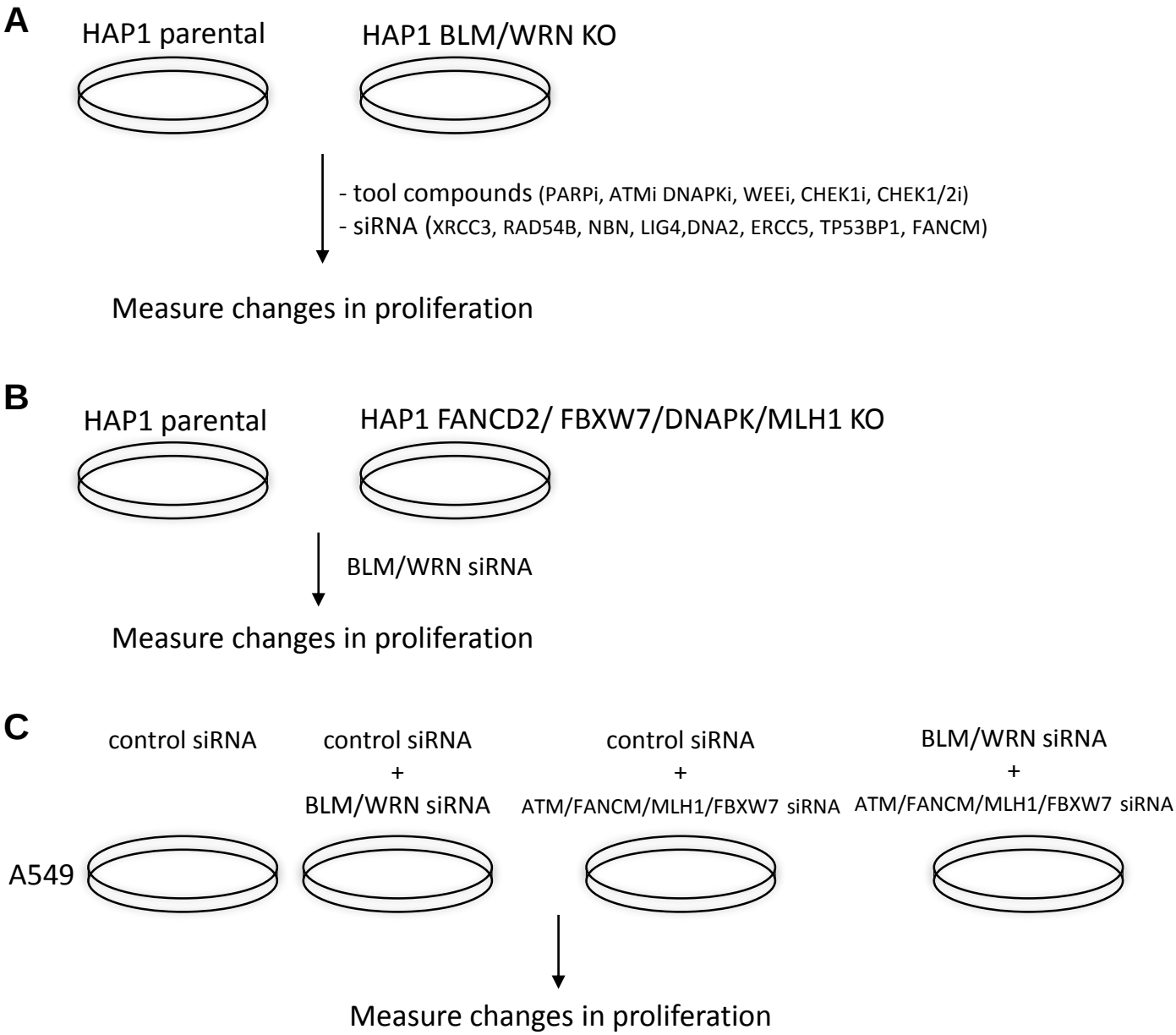

Fig S1. Illustration of experimental approach used to test SL interactions between BLM or WRN and clinically relevant DDR genes. Related to Fig. 1. **A.** HAP1 parental and BLM or WRN KO cells were either treated with tool cmpds or transfected with siRNA. **B.** HAP1 parental and KO cells of potential SL partners were transfected with BLM or WRN siRNA. **C.** Dual siRNA experiments in A549 cells.

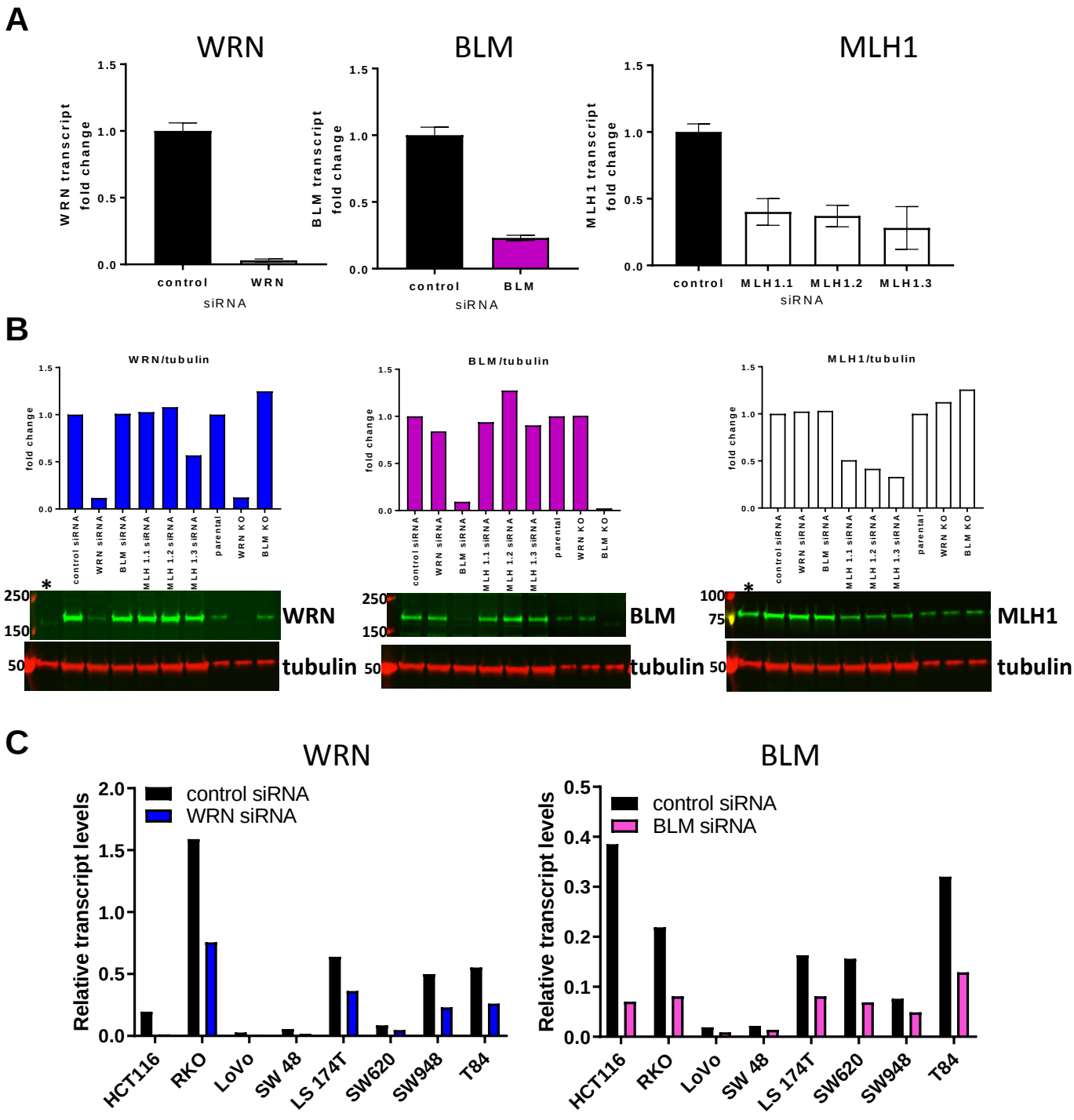

Fig S2. Knockdown efficiency of WRN and BLM siRNAs. Related to Fig. 1. **A**. Transcript knockdown levels in A549 dual siRNA experiments. Error bars represent STDEV. Data are representative of 2 biological experiments. **B.** Protein knockdown levels in A549 dual siRNA experiments and knockout levels in HAP1 isogenic cell lines. Numbers on blots indicate MW bands in kD of protein ladder. * indicates lane loaded with 3X more lysate from HAP1 WRNKO cells. **C.** WRN and BLM transcript levels in CRC cell lines. Data are representative of 2 biological experiments.

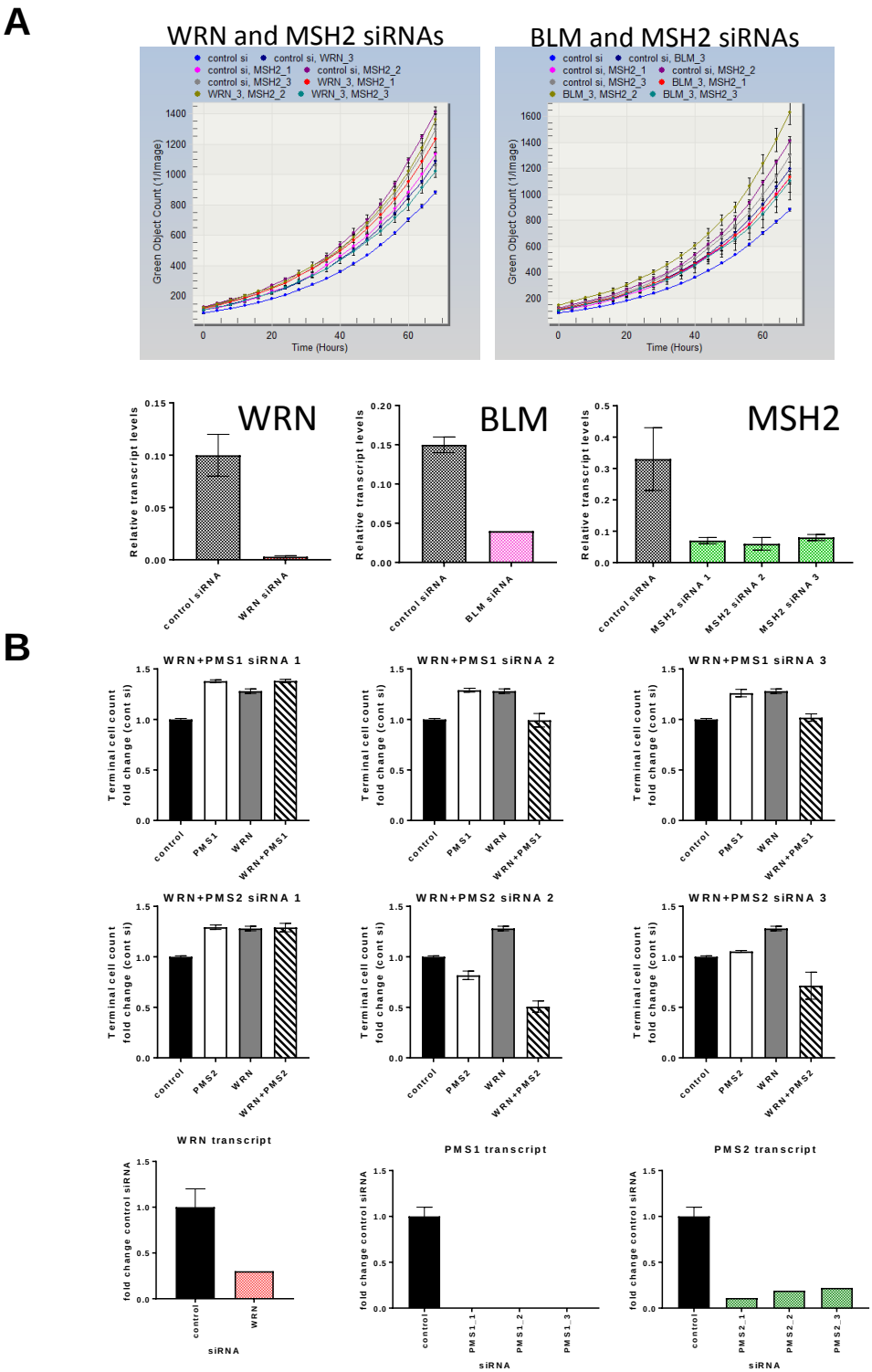

Fig S3. Knockdown of WRN or BLM and other MMR proteins (MSH2, PMS1, PMS2) do not affect the proliferation of A549 cells. Related to Fig. 1. **A.** Proliferation curves following transfection of control, WRN and three independent MSH2 siRNAs (top row). Knockdown levels of WRN siRNA, BLM siRNA and MSH2 siRNAs on WRN transcript, BLM transcript and MSH2, respectively (bottom row). Error bars represent S.E.M. **B.** Terminal cell counts in a 10 day proliferation assays following transfection with control, WRN and three independent PMS1 siRNAs (top row). Terminal cell counts in a 10 day proliferation assay following transfection with control, WRN and three independent PMS2 siRNAs (middle row). Error bars represent S.E.M. Knockdown transcript levels by WRN siRNA, PMS1 siRNAs and PMS2 siRNAs on WRN, PMS1 and PMS2 transcripts, respectively (bottom row). Error bars represent STDEV. Data are representative of 2 biological experiments.

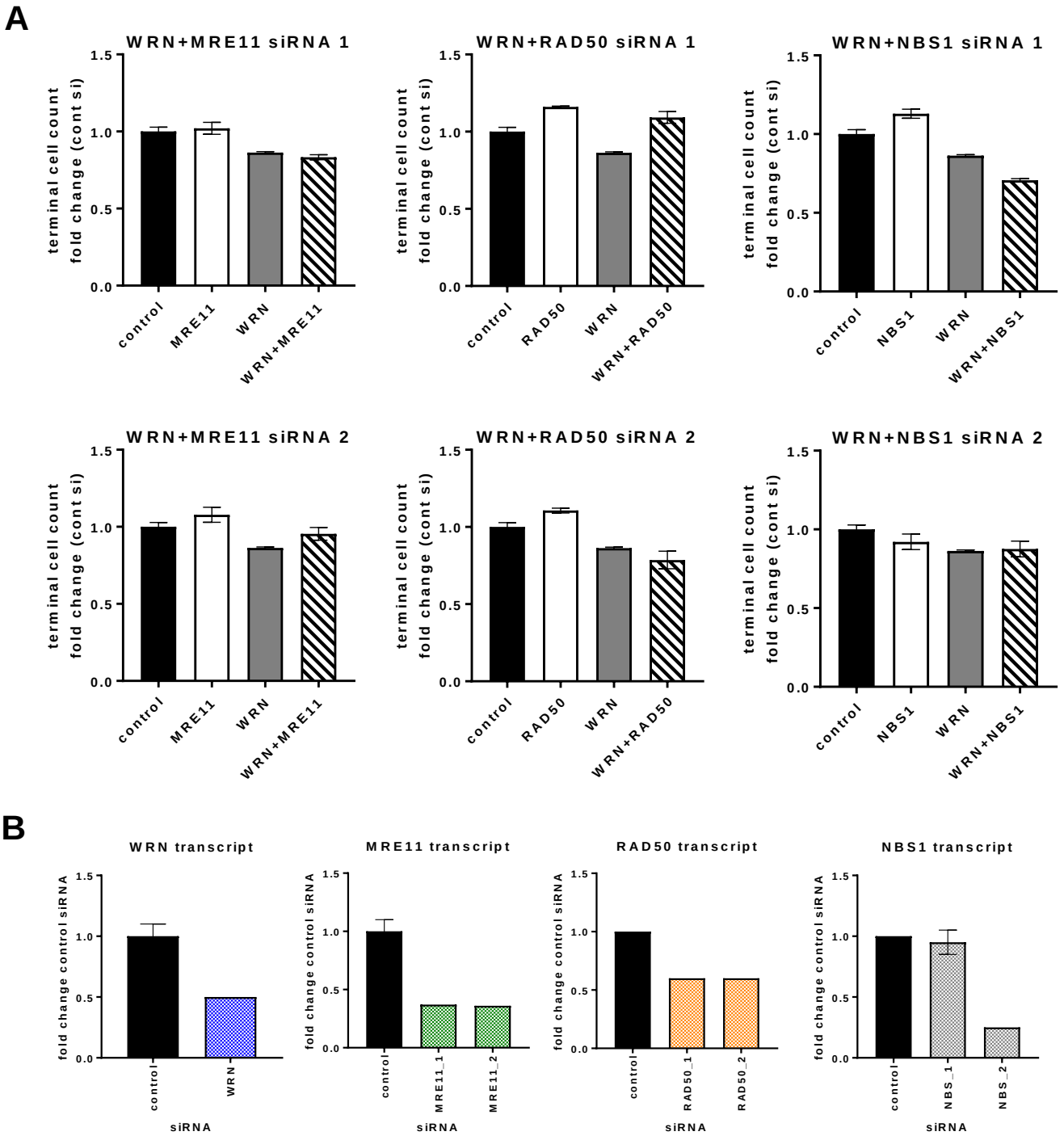

Fig S4. Knockdown of WRN and MRE11, RAD50 or NBS1 do not affect DLD-1 cell proliferation. Related to Fig. 1. **A.** Terminal cell counts in a 10 day proliferation assays following transfection with control, WRN and two independent siRNAs per protein. Error bars represent S.E.M. **B.** Knockdown transcript levels for indicated siRNAs and transcripts. Error bars represent STDEV. Data are representative of 2 biological experiments.

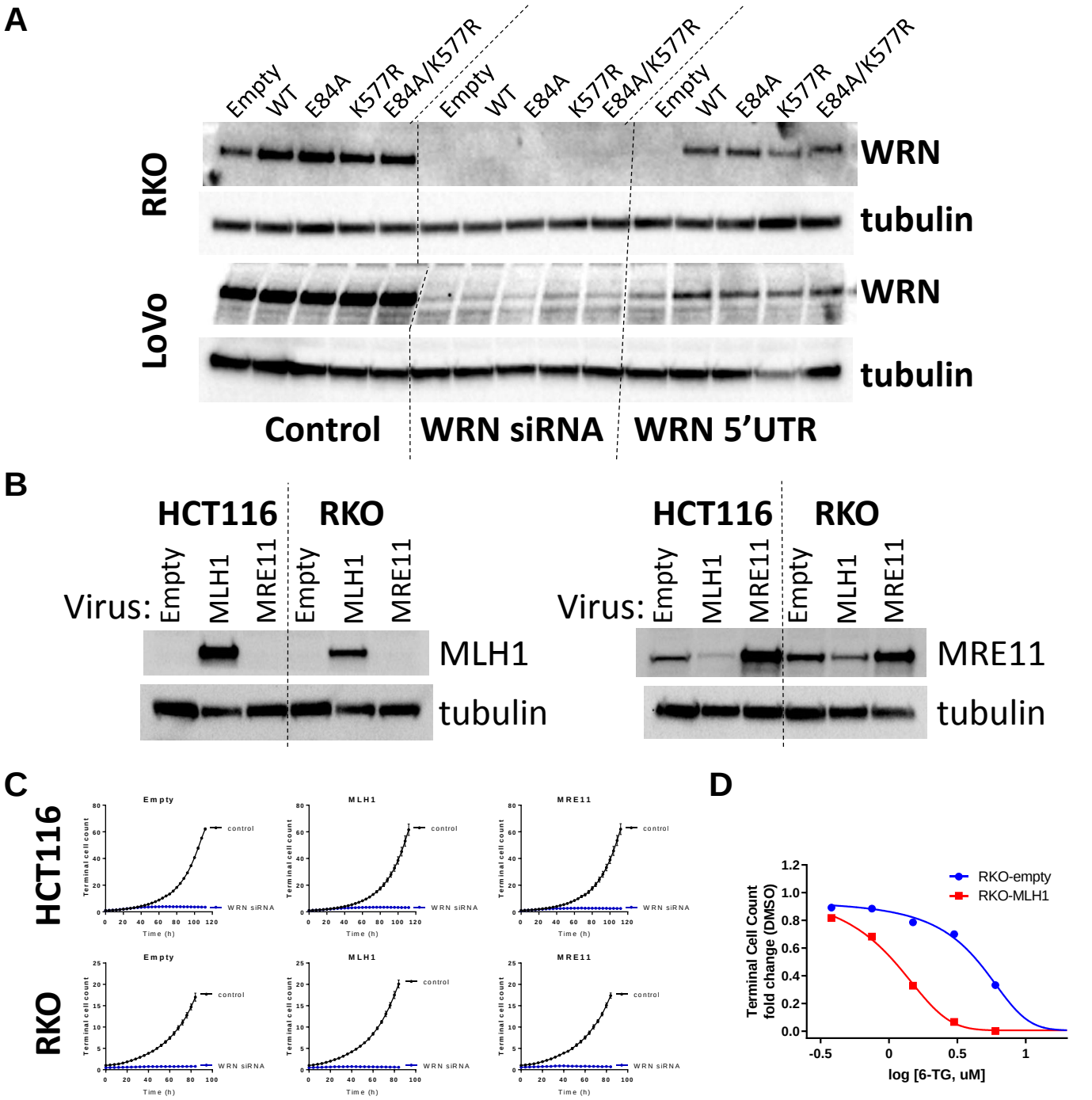

Fig S5.. Rescue experiments of WRN knockdown phenotype in MSI-H cell lines. Related to Fig. 2. **A.** WRN and tubulin immunoblots of RKO and LoVo rescue cell lines transfected with the indicated siRNAs. **B.** MLH1 or MRE11 and tubulin immunoblots of infected HCT116 and RKO rescue cell lines. **C.** Growth curves showing cell number over time of MSI (HCT116, RKO) rescue cell lines transfected with control (black) or WRN (blue line) siRNAs. Error bars represent S.E.M. **D.** Terminal cell count of RKO and RKO+MLH1 4 days after being treated with 6-thioguanine for 24h. Data are representative of 2 biological experiments.

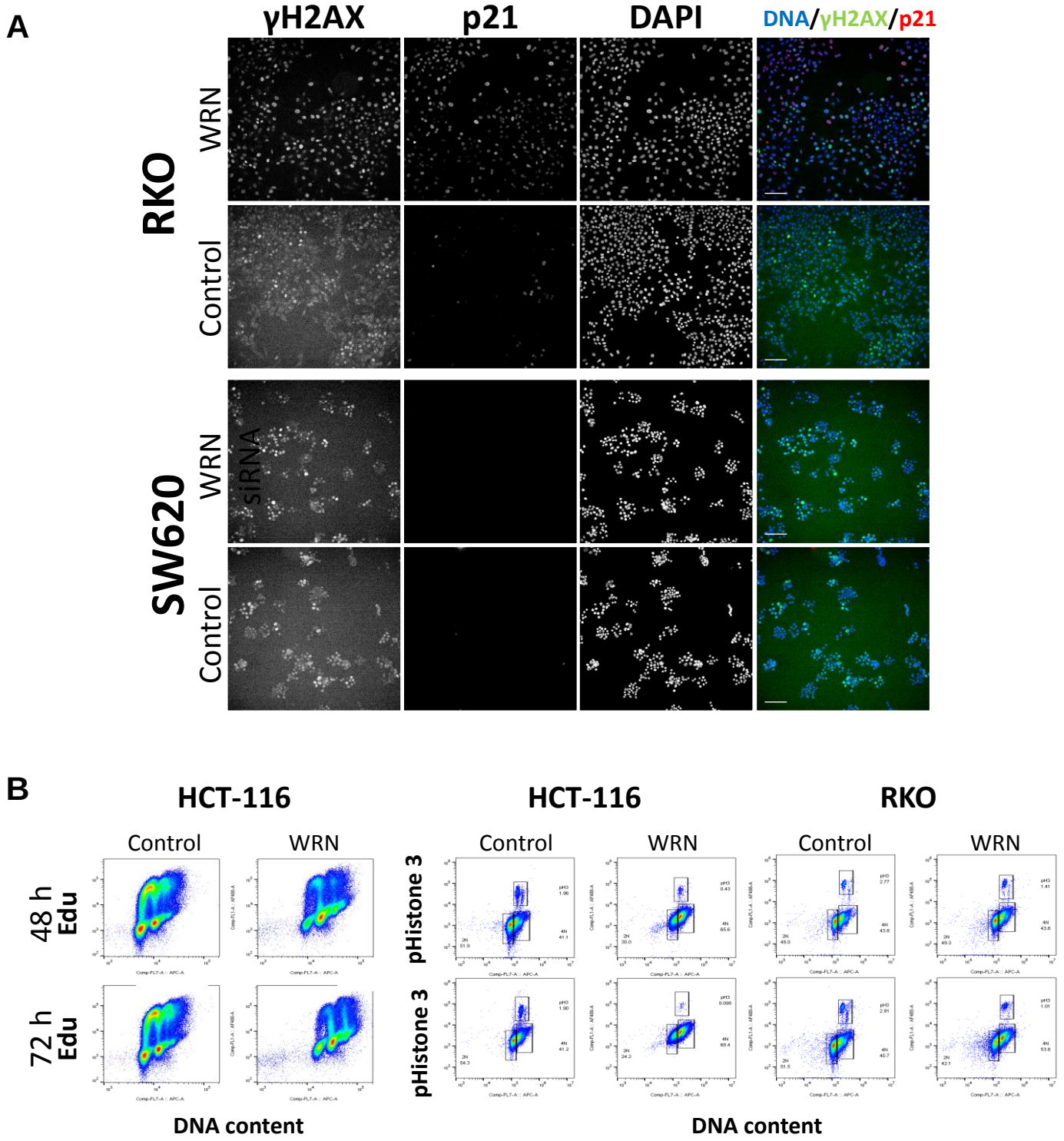

Fig S6. WRN knockdown increases γH2AX and p21 levels and alters the cell cycle of MSI cells. Related to Fig. 3. **A.** Representative immunofluorescence images of RKO and SW620 cells transfected for 72 h with WRN or control siRNAs. Bars, 50 µm. **B.** Scatter plots of MSI cells transfected with control or WRN siRNA following flow cytometry analysis. Edu incorporation in HCT116 cells (left). Phospho-histone 3 antibody staining on HCT116 and RKO cells (right). Data are representative of 2 biological experiments.

TRANSPARENT METHODS:

Cell lines and Reagents

HAP1 isogenic cell lines were obtained from Horizon Discovery (BLM; HZGHC000629c007, WRN; HZGHC000432c001). All other lines were obtained from ATCC. Stable cell lines were generated using lentiviral infection by cloning into a pLVbsd-EF1a-HA vector. Cloning and lentiviral particle generation were carried out at Biosettia Inc. Cells were seeded into a 6-well plate (225,000 cells/well). After 24 h, cells were infected with the virus in the presence of polybrene (8 µg/ml) at a MOI of 5 for WRN rescue experiments and MOI of 10 for MLH1 and MRE11 rescue experiments. Approximately 48 h later, cells were selected in a medium containing 10 µg/ml of blasticidin. Antibodies were obtained from the following vendors: WRN (Bethyl labs; A300-239A), Tubulin (Li-COR; 926-42211), γH2AX (Millipore; 05-636), p21 (abcam; ab109520), phospho-H3 488 (Cell signaling; 3465S).

Transfections

siRNAs were obtained from Life technologies.

Gene	siRNA ID#	Antisense sequence
WRN	s14907	AGUAAGAUAGAAACCCUCCgt
WRN 5'UTR	NM_000553_stealth_691	AAACCCGAGAAGAUCCAGUCCAACA
BLM	s1999	UUUCGUUUUGGAAGAUAUCtt
MLH 1.1	s297	AUAUUGUCCACGGUUGAGGca
MLH 1.2	s298	UAUUGUCCACGGUUGAGGCat
MLH 1.3	s224048	UAUCCUCACAUCCAAUUUCta
MSH2 1.1	s8966	UUACACGAAAGUAAUAUCCaa
MSH2 1.2	s8967	UAAGAUCUGGGAAUCGACGaa
MSH2 1.3	s8968	UAUCAUAUCCUUGCGAUUCtc
PMS1 1.1	s229950	UCUACAUUCAUAAACUUCCtt
PMS1 1.2	s229951	ACAAGUUUUACUAUAUUCCgt
PMS1 1.3	s229952	UCUUUUAAAUCUGCUACUCca
PMS2 1.1	s10740	AUUGGUGCAACUUACACGGat
PMS2 1.2	s10742	AAACUCGAAAUUUACAUCCgg
PMS2 1.3	s534928	UCUUGUAGCAAAAUUUGCCtt
Kif11	s7903	UGAACUUAGAAGAUCAGUCtt

Cells were transfected with 5 nM of negative control siRNA # 1 (catalog# 4390842) or relevant siRNA. Cells were counted and seeded into a 24-well plate (50,000-75,000 cells/well). Approximately 8 h later, they were transfected with siRNA. After 3-4 days, the control siRNA transfected cells were counted and seeded into a 96-well plate (500-1000 cells/well) in triplicate. The remaining cells were used to determine knock down levels using RTPCR. Gene-targeting siRNA transfected cells were seeded using the volume calculated for the control siRNA cells to maintain the effects that occurred during the first 4 days of knockdown. The next day, the cells were transfected again and monitored over 4-5 days in an IncuCyte ZOOM live cell analysis instrument.

Western Blots

100 µl of 1X RIPA plus 6M UREA lysis buffer was added to cells in 1 well of a 24-well plate. The lysate was then transferred to an Eppendorf tube and sonicated. Supernatant following centrifugation at max speed for 10 mins, was transferred to a PCR plate contain the appropriate volume of 6X loading dye. The samples were then heated for 10 mins at 85 degrees. 10-20 µl of resulting lysate was added to one lane of a SDS-Page gel using Precision Plus Protein Dual Color Standard ladder (Biorad; 1610374) to determine MW. Following transfer to nitrocellulose membranes, membranes were cut at relevant MW and incubated with primary antibodies (1:1000) overnight and then horse radish peroxidase (HRP)- or infrared (IR)- conjugated secondary antibodies (1:20,000) for 30 mins. Blots were imaged using ChemiDoc or LI-COR Odyssey instruments for HRP or IR-detection methods, respectively.

RT-PCR

Taqman Probes were obtained from Life technologies. RNA was isolated using an RNAeasy purification kit (Qiagen; 74106). 100 ng of RNA was used in a reverse transcription reaction (Life technologies; 11756500). The resulting cDNA was diluted two-fold and added to taqman gene expression master mix (Life technologies; 4369016) containing the internal gene control probe against PPIA (VIC) and target gene probe (FAM) following the vendor's manual.

Gene	Probe ID
WRN	Hs00172155
BLM	Hs00172060
MLH1	Hs00979919
MSH2	Hs00953527
PMS1	Hs00922262
PMS2	Hs00241053
PPIA	Hs04194521

Immunofluorescence

Cell were seeded into 96-well plates (2000 cells/well), transfected 24h, 48h and 72h prior to being fixed with 3.7% formaldehyde. 0.5% Triton-X was used to permeabilize the cell prior to blocking with SuperBlock buffer (ThermoFisher; 37515) for 0.5 h. Cells were incubated with primary antibodies overnight, washed and then incubated for 0.5 h with secondary antibodies and Hoechst dye. Four images per well were collected and analyzed using a high-content INCell analyzer imaging system and software, respectively.

Flow cytometry

Cell were seeded into 6-well plates (100,000-150,000 cells/well), transfected at 48h and 72h. To detect cells in S-phase, we used a Click-iT EdU kit (Life technologies; C10425). Cell were incubated for 2h with 10 µM EdU. To detect cells in M phase, transfected cells were fixed with 3.7% formaldehyde, permeabilized with 0.5% Triton-X and incubated with an anti-phospho H3 antibody after blocking with SuperBlock buffer (ThermoFisher; 37515) for 0.5 h. To measure DNA content, DRAQ7 (Abcam; ab109202) was added to the cells prior to analysis.

Proliferation assays

Cells were infected with NucLight Red lentivirus (Essen Biosciences; 4476) to express a red fluorescent protein in the nucleus thus enabling live-cell counting. 50,000 cells were infected with the virus at an MOI of 0.5. To eliminate uninfected cells, cells were grown in media containing puromycin (2 µg/ml).

NucLight Red cells were counted, transfected with siRNA and monitored for 4 d in an IncuCyte ZOOM instrument. To measure caspase activity, cells were split into media containing CellEvent reagent diluted 1:1000 (Invitrogen; C10423).

For chemical inhibitor treatment, cells were seeded at 500 cells/well into a 96-well plate and treated the next day with inhibitors for 4 days. PARP, WEE1 and CHEK inhibitors were used at the following concentrations: 0.1, 0.5 and 1 µM. DNAPK and ATM inhibitors were used at the following concentrations: 1, 5 and 10 µM.